

Zero Voltage Switching Of Boost Converter with High Voltage Gain

J Saravanan*, S Sahaya Elsi**

*(Department of Electronics and Communication Engineering, University college of Engineering, Nagercoil – 629004)

** (Department of Electronics and Communication Engineering, University college of Engineering, Nagercoil – 629004)

ABSTRACT

A soft-switching dc/dc converter with high voltage gain is proposed in this paper. It provides a continuous input current and high voltage gain with low current ripples. Moreover, zero voltage switching characteristic of the proposed converter reduces switching loss of active power switches and raises the conversion efficiency. The reverse-recovery problem of output rectifiers is also alleviated by controlling the current changing rates of diodes with the use of the leakage inductance of a coupled inductor.

The converter produces 360V DC output from a 24V DC input. Simulation was carried out with the MATLAB/Simulink software and the waveforms were obtained. The same circuit was also simulated using Power Simulator software (PSIM) and the waveforms were obtained and both the simulated values were compared.

Keywords – Boost Converter, Low Current Ripple, Zero Voltage Switching

I. INTRODUCTION

Nowadays, the demand for dc/dc converters with high voltage gain [1] has increased. The power shortage and the atmosphere pollution have led to more researches on the renewable and green energy sources such as the solar arrays and the fuel cells. Moreover, the power systems based on battery sources and super capacitors have been increased. Unfortunately, the output voltages of these sources are relatively low. Therefore, the step-up power conversion is required in these systems. Besides the step-up function, [3] the demands such as low current ripple, high efficiency, fast dynamics, light weight, and high power density have also increased for various applications. Input current ripple is an important factor in a step-up dc/dc converter. Especially in the fuel cell systems, reducing the input current ripple is very important because the large current ripple shortens fuel cell's [2] lifetime as well as decreases performance. Therefore, current-fed converters are commonly used due to their ability to reduce the current ripple.

Battery powered systems often stack cells in series to achieve higher voltage. However, sufficient stacking of cells is not possible in many high voltage applications due to lack of space. Boost converters [3] can increase the voltage and reduce the number of cells. Two battery-powered applications that use boost converters are hybrid electric vehicles (HEV) and lighting systems.

The NHW20 model Toyota Prius HEV uses a 500 V motor. Without a boost converter, the Prius would need nearly 417 cells to power the motor.

However, a Prius actually uses only 168 cells and boosts the battery voltage from 202 V to 500 V. A white LED typically requires 3.3 V to emit light, and a boost converter can step up the voltage from a single 1.5 V alkaline cell to power the lamp. Boost converters can also produce higher voltages to operate cold cathode fluorescent tubes (CCFL) in devices such as LCD backlights and some flashlights.

A boost converter is used as the voltage increase mechanism in the circuit known as the 'Joule thief'. This circuit topology is used with low power battery applications, and is aimed at the ability of a boost converter [9] to 'steal' the remaining energy in a battery. This energy would otherwise be wasted since the low voltage of a nearly depleted battery makes it unusable for a normal load. This energy would otherwise remain untapped because many applications do not allow enough current to flow through a load when voltage decreases. This voltage decrease occurs as batteries become depleted, and is a characteristic of the ubiquitous alkaline battery. Since $(P=V^2/R)$ as well, and R tends to be stable, power available to the load goes down significantly as voltage decreases.

II. BLOCK DIAGRAM

Figure (1) shows the block diagram of the proposed converter.

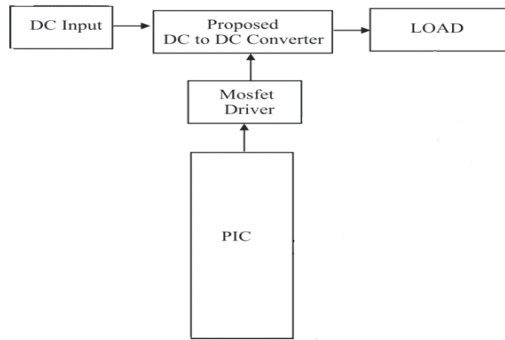


Fig. (1)

In applications that require a voltage step-up function and a continuous input current, a continuous-conduction-mode (CCM) boost converter is often used due to its advantages such as continuous input current [8] and simple structure. However, it has a limited voltage gain due to its parasitic components. Moreover, the reverse-recovery problem [5] of the output diode degrades the system's performance. At the moment when the switch turns on, the reverse-recovery phenomenon of the output diode of the boost converter is provoked. The switch is submitted to a high current change rate and a high peak of reverse-recovery current. The parasitic inductance that exists in the current loop causes a ringing of the parasitic voltage, and then, it increases the voltage stresses of the switch and the output diode. These effects significantly contribute to increase switching losses and electromagnetic interference. The reverse-recovery problem [5] of the output diodes is another important factor in dc/dc converters with high voltage gain. In order to overcome these problems, various topologies have been introduced. In order to increase the voltage gain, the boost converters with coupled inductors are proposed. Their voltage gains are increased, but they lose a continuous input current characteristic and the efficiency is degraded due to hard switching of power switches. For a continuous input current, current-fed step-up converters are proposed [3]. They provide high voltage gain and galvanic isolation.

However, the additional snubbers are required to reduce the voltage stresses of switches. In order to increase the efficiency and power conversion density, a soft-switching technique [8] is required in dc/dc converters. A soft-switching dc/dc converter with high voltage gain is proposed [1]. A CCM boost cell provides a continuous input current [8]. To increase the voltage gain, the output of the coupled inductor cell is laid on the top of the output of the CCM boost cell. Therefore, high voltage gain is obtained without high turn ratio of the coupled inductor, and the voltage stresses of the switches are confined to the output voltage of the CCM boost cell. A zero-voltage-switching (ZVS) operation [8] of the power switches reduces the switching loss during the switching transition and improves the overall efficiency. The

theoretical analysis is verified by an experimental prototype with 24V-to-360 V conversion.

III. CIRCUIT DIAGRAM

A soft-switching dc/dc converter with high voltage gain, which is shown in Figure (2), is proposed. A CCM boost cell provides a continuous input current. To increase the voltage gain, the output of the coupled inductor cell is laid on the top of the output of the CCM boost cell. Therefore, the high voltage gain is obtained without high turn ratio of the coupled inductor, and the voltage stresses of the switches are confined to the output voltage of the CCM boost cell.

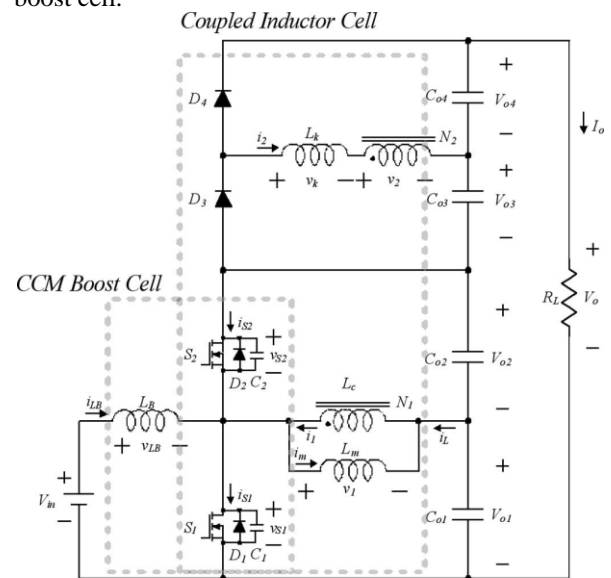


Fig. (2)

A zero-voltage-switching (ZVS) operation of the power switches reduces the switching loss during the switching transition and improves the overall efficiency. The theoretical analysis is verified by a 200 W experimental prototype with 24-to-360 V conversion.

IV. ANALYSIS

The DC/DC boost converter only needs four external components: Inductor, Electronic switch, Diode and output capacitor. The converter can therefore operate in the two different modes depending on its energy storage capacity and the relative length of the switching period. The two operating modes are known as the Discontinuous Conduction Mode (DCM) and Continuous Conduction Mode (CCM), corresponding to the cases with and without an idling interval respectively.

I.

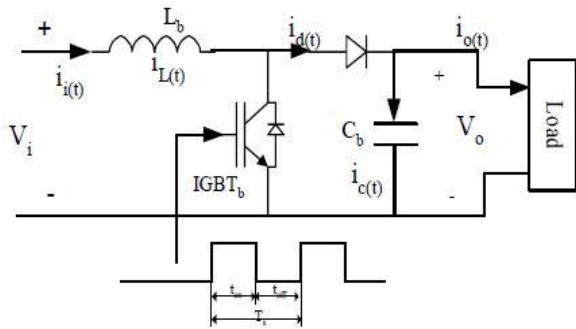


Fig. (3)

4.1. CONVERSION MODES

The DC/DC converter has two modes, a Continuous Conduction Mode (CCM) for efficient power conversion and Discontinuous Conduction Mode (DCM) for low power or stand-by operation.

4.1.1 CONTINUOUS CONDUCTION MODE

Mode 1 (0 < t ≤ ton)

Mode 1 begins when IGBT is switched on at t = 0 and terminates at t = ton. The equivalent circuit for the mode 1 is shown in Fig. 3.1 (a). The inductor current iL(t) is greater than zero and ramp up linearly. The inductor voltage is Vi.

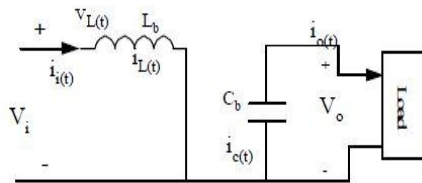


Fig.3.1 (a)

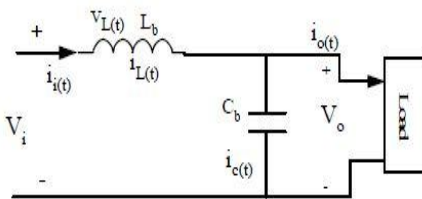


Fig. 3.1 (b)

Mode 2 (ton < t ≤ Ts)

Mode 2 begins when IGBT is switched off at t = ton and terminates at t = Ts. The equivalent circuit for mode 2 is shown in Fig. 3.1 (b). The inductor current decrease until the IGBT is turned on again during the next cycle. The voltage across the inductor in this period is

$$V_i - V_o \cdot V_i t_{on} + (V_i - V_o) t_{off} = 0 \tag{1}$$

Where

Vi : The input voltage.

Vo : The average output voltage.

ton : The on period of IGBT

toff : The off period of IGBT

Dividing both sides by Ts and rearranging items yield

$$\frac{V_o}{V_i} = \frac{T_s}{t_{off}} = \frac{1}{(1-D)} \tag{2}$$

Where

Ts: The switching period.

D: The duty cycle.

Thus, Vo is inversely proportional to (1-D). It obvious that the duty cycle, D, cannot be equal to 1 otherwise there would be no energy transfer to the output. Assuming a lossless circuit, then Pi=Po

$$I_i V_i = I_o V_o \tag{3}$$

$$\frac{I_o}{I_i} = (1-D) \tag{4}$$

Where

I0 : The average output current, Amp.

Ii : The average input current, Amp.

4.1.2 DISCONTINUOUS CONDUCTION MODE

If the current flowing through the inductor falls to zero before the next turn-on of the switching IGBT, then the boost converter is said to be operating in the discontinuous conduction mode. If we equate the integral of the inductor voltage as shown in Fig.3.2 (c) over one time period to zero,

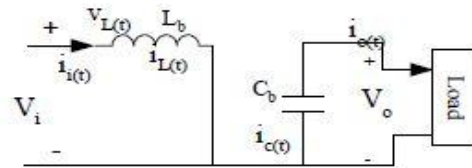


Fig.3.2 (a)

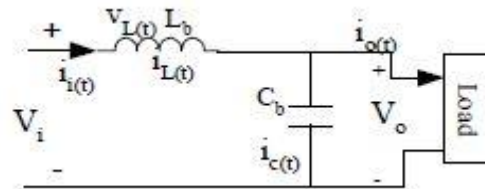


Fig.3.2 (b)

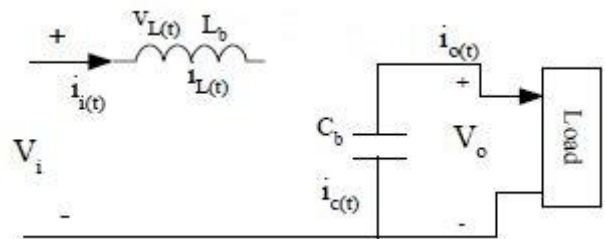


Fig.3.2 (c)

(a) Mode 1 (0 < t ≤ ton) (b) Mode 2 (ton < t ≤ (D+D1)Ts) (c) Mode 3 (D+D1)Ts < t ≤ Ts

$$V_i D T_s + (V_i - V_o) D_1 T_s = 0 \tag{5}$$

$$\frac{V_o}{V_i} = \frac{D+D_1}{D_1} \tag{6}$$

$$\frac{I_o}{I_i} = \frac{D+D_1}{D} \tag{7}$$

From Fig.3.2 (c), the average input current, which is equal to the inductor current, is

$$I_i = \frac{V_i}{2L_h} D T_s (D+D_1) \tag{8}$$

Using above Equ in the foregoing equation yields

$$I_0 = \left(\frac{V_1}{2L_b} T_s\right) DD1 \quad (9)$$

In practice, since V_0 is held constant and D varies in response to variation in V_i , it is more useful to obtain the required duty cycle, D , as a function of load current for varies values of V_0/V_i . By using Eqns (6) and (9), we can determine that:

$$D = \left[\frac{4}{27} \frac{V_0}{V_i} \left(\frac{V_0}{V_i} - 1 \right) \frac{I_0}{I_{0,aver,max}} \right]^{0.5} \quad (10)$$

The maximum average output current at the edge of continuous conduction and can be found by the following Equation.

$$I_{0,aver} = \frac{T_s V_0}{2L_b} D (1 - D)^2 \quad (11)$$

The average output current has its maximum at $D=1/3$.

$$I_{0,aver,max} = \frac{2}{27} \frac{T_s V_0}{L_b} \quad (12)$$

The critical inductance, L_{bc} , is defined as the inductance at the boundary edge between continuous and discontinuous modes and is defined as:

$$L_{bc} = \frac{RD(1-D)^2}{2F_s} \quad (13)$$

Where

R: The resistive load

F_s : The switching frequency

The switching frequency has been chosen arbitrarily to minimize the size of the boost inductor and limit the loss of the semiconductor device. At higher frequencies the switching losses in the IGBT increase, and therefore reduce the overall efficiency of the circuit. At lower frequencies the required output capacitance and boost inductor size increases, and the volumetric efficiency of the supply degrades.

V. DESIGN PARAMETERS

5.1. Ripple current

The input current ripple ΔI_{LB} can be written as

$$\Delta I_{LB} = I_{LB1} - I_{LB2} = \frac{DV_{in} T_s}{L_B} \quad (14)$$

To reduce the input current ripple ΔI_{LB} below a specific value I^* , the inductor L_B should satisfy the following condition:

$$L_B > \frac{DV_{in} T_s}{I^*} \quad (15)$$

5.2. Voltage gain

The voltage gain of the proposed converter is obtained by

$$\frac{V_0}{V_{in}} = \frac{1}{1-D} = \frac{nD(1-\alpha)}{(D-\alpha(2D-1))(1-D+\alpha(2D-1))} \quad (16)$$

On the assumption that α is small the voltage gain is simplified as

$$\frac{V_0}{V_{in}} = \frac{1+n}{1-D} \quad (17)$$

5.3. ZVS Condition

The ZVS condition for S_2 is given by,

$$I_{m2} + nI_{D3} + I_{LB1} > 0 \quad (18)$$

From where, it can be seen that the ZVS of S_2 is easily obtained. For ZVS of S_1 , the following condition should be satisfied:

$$I_{m1} + nI_{D4} > I_{LB2} \quad (19)$$

On the assumption that α is small, I_{D4} and I_{LB2} can be simplified as follows

$$I_{D4} = \frac{2I_0}{1-D} \quad (20)$$

$$I_{LB2} = \frac{(n+1)I_0}{1-D} = \frac{\Delta I_{LB}}{2} \quad (21)$$

From (20) and (21), the inequality (19) can be rewritten by

$$I_{m1} + \frac{2nI_0}{1-D} > \frac{(n+1)I_0}{1-D} - \frac{\Delta I_{LB}}{2} \quad (22)$$

Since I_{m1} , I_0 and ΔI_{LB} are all positive values, the inequality (22) is always satisfied for $n>1$.from (18) and (22) it can be seen that ZVS conditions for S_1 and S_2 are always satisfied.

VI. SIMULATION CONCEPT

The proposed converter produces 360V dc output voltage from a 24V dc input voltage. The 24V dc input voltage is fed from the dc input source. The 24V is passed through the base inductance L_b and then through the MOSFET switches S_1 and S_2 . Through the switches it was fed through the transformer for the boosting action. Since the output of the transformer is ac, it is fed through the diode D_1 and D_2 for the rectifying action. Then finally the rectified voltage is given to the resistive load. The scope across the voltage and current measurement will provide the necessary graphs for the output voltage indicating a magnitude of 360V and the continuous output current. Similarly the scope across the switches will provide the voltage and current waveforms.

VII. OUTPUT WAVEFORMS

7.1. Output voltage using PSIM

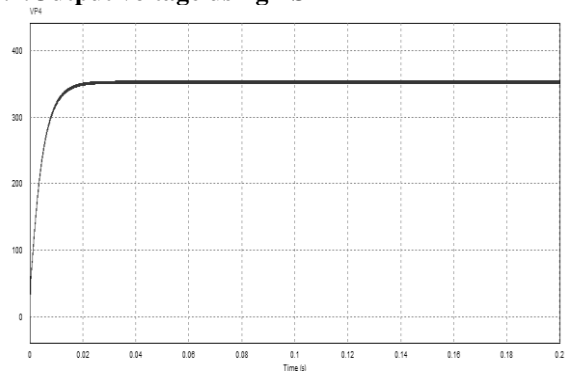


Fig.4

Figure (4) shows the output voltage waveform of a Power Simulator.

7.2. Output current using PSIM

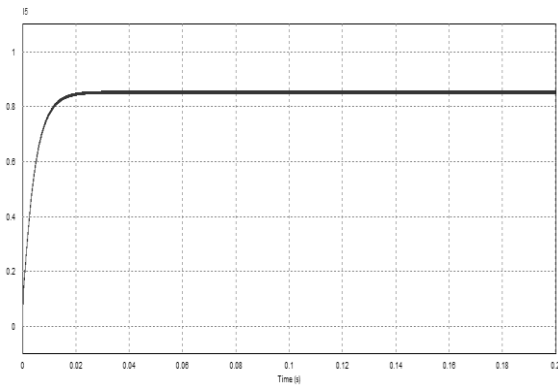


Fig.5

Figure (5) shows the output current waveform of a Power Simulator.

7.3. Output voltage using MATLAB

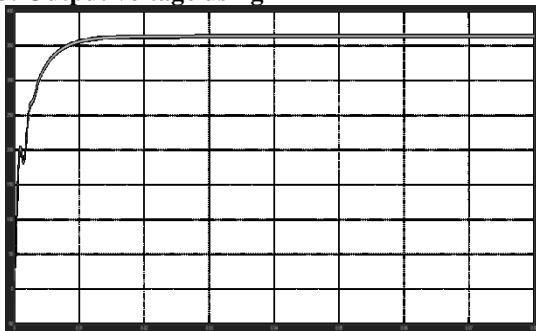


Fig.6

Figure (6) shows the output voltage waveform of a Matlab.

7.4. Output current using MATLAB

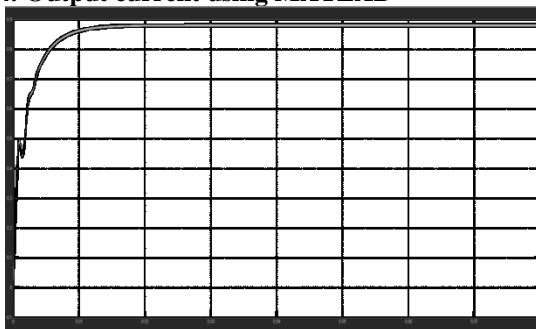


Fig.7

Figure (7) shows the output current waveform of a Matlab.

VIII. EXPERIMENTAL RESULTS

The prototype soft-switching dc/dc converter with high voltage gain is implemented with specifications of $n = 5$, $V_{in} = 24V$, $V_o = 360 V$, $L_B = 154 \mu H$, $L_k = 74 \mu H$, $C_{o1} = C_{o2} = C_{o3} = C_{o4} = 47 \mu F$, $L_m = 105 \mu H$, $f_s = 100 \text{ kHz}$, and $P_o = 200 \text{ W}$.

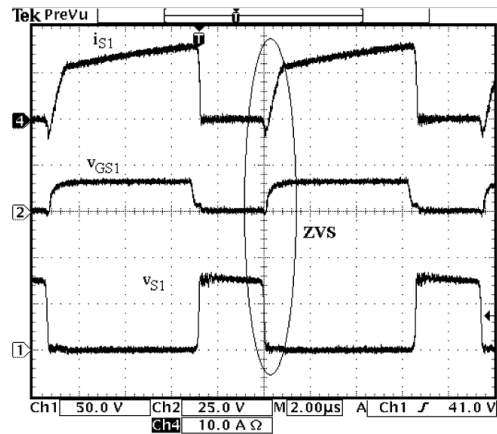
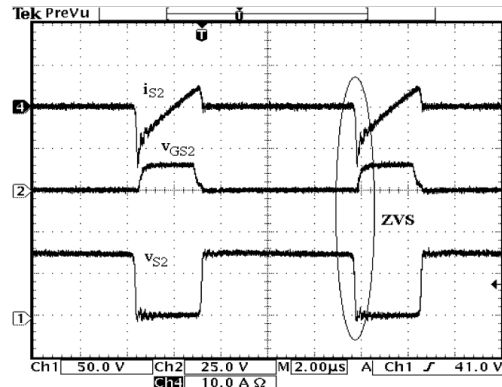


Fig. 8

Figure (8) shows the experimental results of the proposed converter.



IX. MATLAB AND PSIM COMPARISON

Parameter	MATLAB Simulation	PSIM Simulation
Building the model	Complicated	Simple
Simulation time	Large time	Less time
Functionality	Multi functional	Less functional
Output voltage V_o	364.17V	352.1V
Output current I_o	0.8831A	0.8523A

Table.1

Table (1) shows the comparison between Matlab and Power Simulator.

X. CONCLUSION

A soft-switching dc/dc converter with high voltage gain has been proposed in this paper. The proposed converter can minimize the voltage stresses of the switching devices and lower the turn ratio of the coupled inductor. It provides a continuous input current, and the ripple components of the input current can be controlled by using the inductance of the CCM boost cell. Soft switching of power switches and the

alleviated reverse-recovery problem of the output rectifiers improve the overall efficiency.

REFERENCES

- [1] "A Soft-Switching DC/DC Converter with High Voltage Gain" Hyun-Lark Do. *IEEE transactions on power electronics*, vol. 25, no. 5, may 2010.
- [2] S. K. Mazumder, R. K. Burra, and K. Acharya, "A ripple-mitigating and energy-efficient fuel cell power-conditioning system," *IEEE Trans. Power Electron.*, vol. 22, no. 4, pp. 1437–1452, Jul. 2007.
- [3] Z. Qun and F. C. Lee, "High-efficiency, high step-up DC–DC converters," *IEEE Trans. Power Electron.*, vol. 18, no. 1, pp. 65–73, Jan. 2003.
- [4] W. Choi, P. N. Enjeti, and J. W. Howze, "Development of an equivalent circuit model of a fuel cell to evaluate the effects of inverter ripple current," in *Proc. IEEE APEC*, 2004, vol.1, pp.355–361
- [5] Q. Zhao, F. Tao, F. C. Lee, P. Xu, and J. Wei, "A simple and effective method to alleviate the rectifier reverse-recovery problem in continuous current mode boost converter," *IEEE Trans. Power Electron.*, vol. 16, no. 5, pp. 649–658, Sep. 2001.
- [6] J. P. Rodrigues, S. A. Mussa, M. L. Heldwein, and A. J. Perin, "Threelevel ZVS active clamping PWM for the DC–DC buck converter," *IEEE Trans. Power Electron.*, vol. 24, no. 10, pp. 2249–2258, Oct. 2009.
- [7] J. M. Kwon, E. H. Kim, B. H. Kwon, and K. H. Nam, "High-efficiency fuel cell power conditioning system with input current ripple reduction," *IEEE Trans. Ind. Electron.*, vol. 56, no. 3, pp. 826–834, Mar. 2009.
- [8] C. Y. Chiang and C. L. Chen, "Zero-voltage-switching control for a PWM buck converter under DCM/CCM boundary," *IEEE Trans. Power Electron.*, vol. 24, no. 9, pp. 2120–2126, Sep. 2009.
- [9] Y. Hsieh, T. Hsueh, and H. Yen, "An interleaved boost converter with zero-voltage transition," *IEEE Trans. Power Electron.*, vol. 24, no. 4, pp. 973–978, Apr. 2009.
- [10] J. M. Kwon, E. H. Kim, B. H. Kwon, and K. H. Nam, "High-efficiency fuel cell power conditioning system with input current ripple reduction," *IEEE Trans. Ind. Electron.*, vol. 56, no. 3, pp. 826–834, Mar. 2009.
- [11] G. Fontes, C. Turpin, S. Astier, and T. A. Meynard, "Interactions between fuel cells and power converters: Influence of current harmonics on a fuel cell stack," *IEEE Trans. Power Electron.*, vol. 22, no. 2, pp. 670–678, Mar. 2007.